SCIENCE CHINA
Earth Sciences

• RESEARCH PAPER •

October 2014 Vol.57 No.10: 2357–2365
doi: 10.1007/s11430-014-4906-4

Effect of a thermokarst lake on soil physical properties and infiltration processes in the permafrost region of the Qinghai-Tibet Plateau, China

WANG YiBo[1,2,3*], GAO ZeYong[1], WEN Jing[1], LIU GuoHua[1], GENG Di[4] & LI XiaoBing[1]

[1] *College of Earth and Environment Sciences, Lanzhou University, Lanzhou 730000, China;*
[2] *MOE Key Laboratory of Western China's Environmental Systems, Lanzhou University, Lanzhou 730000, China;*
[3] *State Key Laboratory of Frozen Soil Engineering, Cold and Arid Regions Environmental and Engineering Research Institute, Chinese Academy of Sciences, Lanzhou 730000, China;*
[4] *College of Atmospheric Sciences, Lanzhou University, Lanzhou 730000, China*

Received November 26, 2013; accepted March 10, 2014; published online August 4, 2014

Changes in the hydrological processes in alpine soil constitute one of the several key problems encountered with studying watershed hydrology and ecosystem stability against the background of global warming. A typically developing thermokarst lake was chosen as a subject for a study using model simulation based on observations of soil physical properties, infiltration processes, and soil moisture. The results showed that the selected thermokarst lake imposed certain changes on the soil infiltration processes and, with the degree of impact intensifying, the initial infiltration rate decreased. The greatest reduction was achieved in the area of moderate impact. However, the stable infiltration rate and cumulative infiltration gradually increased in the surface layer at a depth of 10 and 20 cm, both decreasing initially and then increasing, which is correlated significantly with soil textures. Moreover, the cumulative infiltration changed in line with steady infiltration rate. Based on a comparative analysis, the Horton model helps better understand the effect on the soil infiltration processes of the cold alpine meadow close to the chosen thermokarst lake. In conclusion, the formation of the thermokarst lake reduced the water holding capacity of the alpine meadow soil and caused the hydraulic conductivity to increase, resulting in the reduction of runoff capacity in the area of the thermokarst lake.

Qinghai-Tibet Plateau, thermokarst lake, soil infiltration, simulation

Citation: Wang Y B, Gao Z Y, Wen J, et al. 2014. Effect of a thermokarst lake on soil physical properties and infiltration processes in the permafrost region of the Qinghai-Tibet Plateau, China. Science China: Earth Sciences, 57: 2357−2365, doi: 10.1007/s11430-014-4906-4

Both natural and human factors cause increases in the depth of seasonal thawing, leading to partial melting of an underground ice layer known as permafrost. The consequent thermal subsidence generates closed depressions in the topsoil, which may generate ponds and larger surface water bodies known as thermokarst lakes (Hinzman et al., 1997). These are distributed mainly in the arctic and subarctic regions of Siberia, Alaska, and Canada as well as in very high mountains found in low latitudes (Lin et al., 2010). The formation of thermokarst lakes can change landforms, permafrost, ecosystems, and the extent of soil erosion in such high and cold regions. In the process of expansion, it can release large amounts of greenhouse gases, thus increasing the global warming trend (Walter et al., 2006; Sergey et al., 2006; Walter et al., 2007).

The Qinghai-Tibet Plateau is a driver or amplifier of global climate change as has been proven by the state of its fragile, extremely sensitive ecological environment in response to climate change and human disturbance (Pan et al.,

*Corresponding author (email: wangyib@lzu.edu.cn)

1996; Ma et al., 2013; He et al., 2013). The permafrost connects with the plateau's energy-water balance, hydrological change, and carbon interchange between the atmosphere and the land surface, as well as the ecosystem and the ecological landscape. Under the impact of human activity and global climate change, the temperature of the permafrost has risen, leading to melting of the underground ice and an increase in the thickness of the active layer (Lin et al., 2009; Johanna et al., 2012; Wu et al., 2013). Some studies have suggested that, in the next 50 years, the permafrost area on the Qinghai-Tibet Plateau will diminish by 8.8% to 13.5% (Nan et al., 2004), active layer thickness increasing further from the current 0.5–1.5 m to 1.5–2.0 m (Guo et al., 2012). Thermokarst lakes are an important factor in permafrost degradation, the distribution of numbers and areas covered showing an increasing trend in the Qinghai-Tibet Plateau. Along the regional railway running from the Kunlun to the Fenghuo mountains, there are more than 250 lakes, with an average size of 5580 m^2 and a total size of 1.39×10^6 m^2 (Niu et al., 2011). The formation of thermokarst lakes can influence soil temperature at the edge of the lake and in its surrounding subsoil, as well as the permafrost table, and obviously influencing temperatures in deeper soils and permafrost thicknesses (Lin et al., 2010). At the same time, the soil environment can also be affected during the drainage process, especially if the soil is shallow (Wang et al., 2011). Based on the available research results, the study of thermokarst lakes has been focused mainly on its impact upon permafrost, the extent of lakeshore erosion, geological disasters, and other issues. However, studies of the surrounding soil environment remain relatively sparse (Kokelj et al., 2013) and, more generally, relevant research on the impact of thermokarst lakes on soil ecological and hydrological processes has not been carried out on the Qinghai-Tibet Plateau.

Based on observations of soil physical properties, soil moisture content and soil infiltration processes distributed in and around thermokarst lakes, this paper aims to clarify the spatial variability of soil moisture and the changes in soil infiltration processes in various affected areas. Emphasis is also placed on the foundations that reveal the influence of variations in the alpine system upon the surface hydrological processes and the soil moisture cycles in the permafrost region, together with research on the permafrost-vegetation-soil moisture coupling relation against the background of global warming (Ren et al., 2013).

1 Material and methods

1.1 Description of the study area

The study area is located in the Wudaoliang Basin where thermokarst lakes are developed typically in the headwaters of the Yangtze River (Figure 1). The average altitude is 4611 m a.s.l., the average annual rainfall 274.7 mm, concentrated mainly in the period from May to September, and the mean air temperature −5.36°C. In short, this area has a typical continental plateau climate throughout the year, having only two seasons (winter and summer). The depth of the active layer is 1.5–2.5 m, with a permafrost thickness of between 30 and 100 m and an average annual soil temperature of −1.0 to −2.0°C. Soil in the study area is classified as the alpine meadow type and the sedimentary strata include deposited layers of the Tertiary lake facies with the Holocene diluvium-alluvial layers of Quaternary (Qh) age. The lithology of the study area consists mainly of mudstone, sandstone, clay, and silt. Finally, where the study area is crossed by a railway and a highway, there are three major alpine vegetation types in the study area, namely, Kobresia meadow, swamp meadow, and forb meadow. Alpine meadow is the dominant vegetation type, with patchy vegetation and sparse vegetation on debris distributed in local high-altitude zones. The dominant plant species in the study area includes *Kobresia pygmaea, K. humilis, K. capillifolia, K. tibetica, Stipaaliena, Potentilla multicaulis,* and *Leontopodium*.

1.2 Methods

A typical and representative thermokarst lake with a relatively circular shape was chosen as the subject of study in the Wudaoliang Basin. The average water depth was ca. 1.3 m. In order to evaluate the impact of lakes and vegetation cover, a standing index of the dominant species of the original cold alpine ecosystem and ecological variability index were used. S_L values were used as a criterion to classify ecosystem variability into five categories: (1) $S_L \geqslant 80$, not-affected; (2) $80 > S_L \geqslant 50$, lightly affected; (3) $50 > S_L \geqslant 30$, medium affected; (4) $30 > S_L \geqslant 20$, severely affected; (5) $S_L < 20$, extremely affected (Wang et al., 2007). We chose three 3 m×3 m quadrats in each of the different affected areas and also investigated the vegetation. Vegetation coverage and distance from the lake is shown in Table 1.

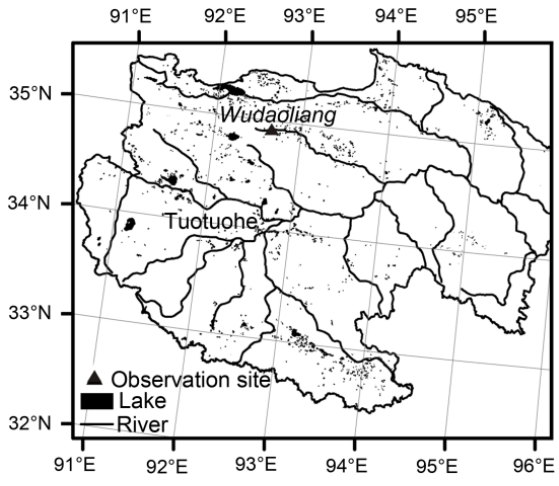

Figure 1 The location of study area.

Table 1 S_L and distance from the lake in different impact degree

S_L (%)	Distance from the lake (m)	Impact degree[a)]
10	9.8	EA
25	10.5	SA
45	13.6	MA
70	16.8	LA
90	31.5	NA

a) NA: Not-affected; LA: lightly affected; MA: medium affected; SA: severely affected; EA: extremely affected.

1.2.1 Measurement of soil properties

In July, 2012, samples were taken in each transect at eight depths with different impact degree (0–5, 5–10, 10–15, 15–20, 20–30, 30–40, 40–50, 50–60 cm). First, three replicate samples were taken using the 100 mL metal ring at each depth and weighed immediately before storing in aluminum boxes. Second, the soil moisture content and bulk density were determined by heating in an oven at 105±2°C. At the same time, soil samples weighing approximately 1 kg were sealed in plastic bags and transported to the laboratory for analysis of soil particle-size composition.

1.2.2 Measurement of soil infiltration processes

Double-ring infiltrometers were used for *in situ* determination of soil infiltration processes, and apparatus testing was undertaken by improved Marriott tube and circular concentric double rings. The Mariotte tube was 180 cm high with a 25.7 cm inner diameter and an outer ring with a diameter of 64.0 cm. The water level in the inner ring was maintained by using the Marriott tube while, in order to ensure one-dimensional flow in the inner ring infiltration, the water level in the outer ring was adjusted manually to match that in the inner ring. The content of supply water was measured by the use of a calibration pipe which hung in the outer ring of the Marriotte tube. We chose an initial 1-min infiltration rate, followed by monitoring at 5-min intervals the rate of fall in the water level within the Mariotte tube. The criterion used for attaining stable-state infiltration was 5-min infiltration volumes that remained constant at four time intervals.

In order to reveal soil infiltration processes at different depths of the vegetation roots, we maintained a fixed water level. Considering soil structure impact on infiltration at the same time (within 1–2 m), we chose three plots to test in different affected areas. Before the surface soil infiltration processes were measured, we removed the litter, leaves, etc. Also, it was necessary to remove the overlying soil before any other soil layers were measured (10, 20 cm). The field measurements are shown in Figure 2.

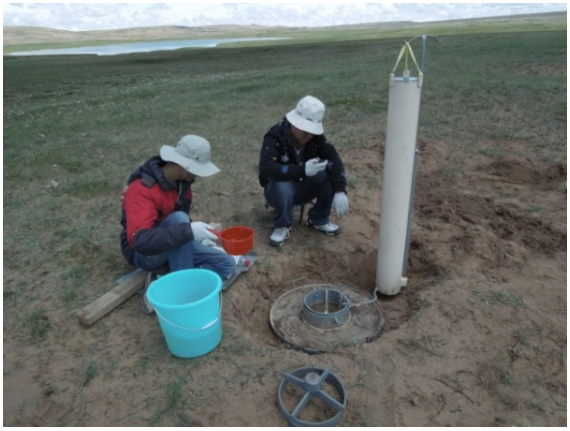

Figure 2 The experiment of soil water infiltration processes.

2 Results and discussion

2.1 Variation in soil physical properties

Since the formation of the thermokarst lake, it has clearly been altered. Notably, the main factors involved the lateral water-heat conductivity of the surrounding soils and the intensity of soil freeze-thaw erosion, together with the coupling effect of cold alpine vegetation, have all impacted upon the physical properties of the soil. As shown in Table 2, in view of the intensification of impact, soil moisture content in the EA (extremely affected) area was just 36.7% compared to the NA (not-affected) area at a depth of between 0 and10 cm. Due to the distribution of dense plant roots in the NA area, the soil bulk density is relatively low. When degraded plant roots of alpine vegetation gradually decay and diminish, causing soil bulk density to increase with the degree of impact intensifying, soil porosity also undergoes a gradual reduction, being only 44.94% in the EA area. With the degree of impact intensifying, while the content of clay and silt decreases, the content of sand obviously increases. At a depth of 10–20 cm, soil moisture content also decreases; SA (severely affected) achieved the minimum, which was equivalent to 62.1% of NA. Compared with other affected areas, soil bulk density was higher and the soil porosity content was lower at SA than at EA. Moreover, there was no obvious grading in soil particle size in this layer. At a depth of 20–30 cm, soil moisture content was higher than the overlying soil and SA reached the maximum of 22.26%. Compared with other layers, soil moisture content demonstrated fluctuations at the 20–30 cm depth, which might be related to the diversity of evaporation intensity, infiltration processes, and lateral recharge in different affected areas. The variation in soil bulk density and porosity displayed a similar trend and, in addition, the content of soil clay and silt was very low, although the sand content was higher in EA and the clay content was only 0.24%.

2.2 The variation in soil infiltration processes

Soil water infiltration is a process which refers to water flowing down into a soil body through all or part of the soil surface, followed by storing and changing the soil moisture content, constituting an important link between transfor-

Table 2 Physical characteristics of soil profiles in different affected areas

Soil depth (cm)	Affected degree	Soil moisture (%)	Soil bulk density (g cm^{-3})	Soil porosity (%)	Clay (%)	Silt (%)	Sand (%)
0–10	NA	18.35	1.076	59.40	1.53	6.08	92.39
	LA	11.53	1.211	54.30	1.64	5.78	92.58
	MA	9.07	1.320	50.19	0.81	2.88	94.84
	SA	6.92	1.380	47.92	0.82	3.63	95.55
	EA	6.73	1.459	44.94	0.85	3.72	95.43
10–20	NA	14.76	1.350	49.06	0.97	3.82	94.18
	LA	11.23	1.260	52.45	0.71	3.97	95.32
	MA	10.20	1.329	49.85	0.93	4.24	94.83
	SA	9.17	1.454	45.13	0.97	3.83	95.20
	EA	10.30	1.443	45.54	0.63	3.34	96.03
20–30	NA	21.29	1.256	52.60	0.93	3.54	95.53
	LA	14.04	1.364	48.53	1.19	4.71	94.10
	MA	11.43	1.330	49.81	1.02	4.33	94.65
	SA	22.26	1.479	44.19	0.86	3.55	95.59
	EA	12.02	1.437	45.77	0.24	2.93	96.83

mation of precipitation, runoff, soil moisture, and groundwater (Shen et al., 2008). The numerical value of soil infiltration rates equals the value of water flux through the infiltration interface, which depends mainly on the hydraulic characteristics of the infiltration front. Water potential gradient decreases as the infiltration time lengthens, thus reducing the infiltration rates. Soil crust, mechanical composition, water-stable aggregate distribution, soil bulk density, soil organic matter content, initial soil moisture content, soil temperature, sodium ion content, and soil transection and other features, impact upon the hydraulic characteristics and also play vital roles on soil infiltration capacity (Li et al., 2011). Above all, the soil infiltration process is not a single factor but a result of the comprehensive effect of various kinds of factors.

In the thermokarst lake area, characteristics of the soil infiltration curve show great variability, reflected mainly in the initial infiltration rate, the stable infiltration rate, the time required to reach the stable state, and the shape of the infiltration process curve, as shown in Figure 3. In the thermokarst lake area, soil infiltration rates declined sharply in the first six minutes, and then changed more slowly from 6 to 21 min; the curve became flat after 21 min. Initial soil infiltration rates on the surface showed less variability than at depths of 10 and 20 cm in different affected areas, but stable soil infiltration rates on the surface and at 10 cm depth were more volatile than at the 20 cm depth, whereas soil infiltration processes reached the stable state more easily at a depth of 20 cm compared to all other depths. The results show that there is a significant difference between soil at depths from 0 to 20 cm and those deeper than 20 cm. The main reason for this result is that cold alpine meadow is generally dominated by *Kobresia humilis*, the plant roots and soil organic matter of which are distributed mainly in shallow soil (0–20 cm); in addition, these factors, together with the effect of soil texture, add further complication to the shallow soil infiltration processes.

2.2.1 Variation in soil initial infiltration rates in different affected areas

The variation of soil initial infiltration rates on different affected areas of the thermokarst lake is shown in Figure 4. The results indicate that the trend in the changing soil initial infiltration rates is similar at different depths. At the soil surface, the initial infiltration rates gradually decrease from NA to MA (medium affected) at an amplitude of 24.0%. From MA to EA, soil initial infiltration rates increased at first but then decreased, reaching a maximum of 6.51 mm min^{-1} at EA. At a depth of 10 cm, with the degree of impact intensifying, initial soil infiltration rates display a changing (parabolic) trend , reaching a minimum of 4.03 mm min^{-1} in MA, whereas the initial infiltration rate at EA was just 77.8% compared to NA. At the 20 cm depth, the initial infiltration rates at LA indicated no obvious changes when compared with NA; from LA (lightly affected) to MA, the initial infiltration rates decreased by 33.3%, but they increased by 25.0% from MA to EA. In a word, the formation of the thermokarst lake reduced the initial soil infiltration rates and the greatest amplitude of reduction occurred in the MA area.

Initial soil infiltration rates directly influence the pattern of regional runoff. When rates were lower, surface runoff exceeded infiltration, causing the precipitation recharge of the river channel to run off rapidly. When the rates were higher, precipitation supplied the soil moisture content through the infiltration processes. Thus, studying the initial soil infiltration rates on the area of the thermokarst lake provided a positive means of understanding the runoff mechanism of the Yangtze River, variation of the river channel in relation to global warming, and changes in the alpine soil environment. Tables 2 and 3 show that the variation in initial soil infiltration rates under the influence of the thermokarst lake is a result of coupled multi-factors, closely correlated with the soil moisture content. However, the relation with soil texture was weak. In addition, degradation of

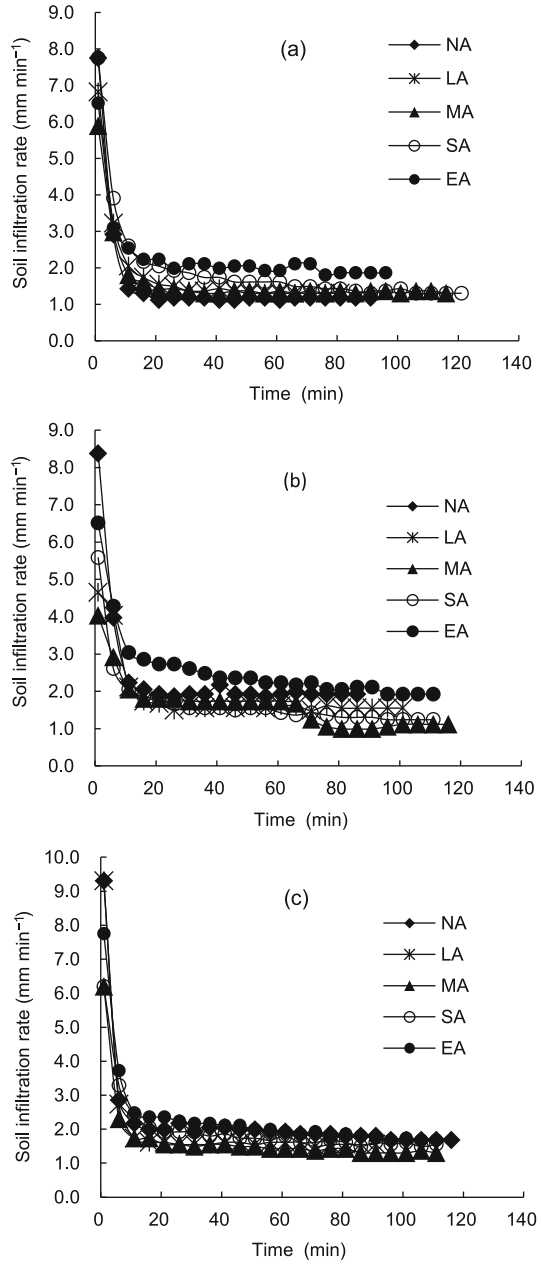

Figure 3 The soil infiltration processes under different influenced degree. (a) 0 cm; (b) 10 cm; (c) 20 cm.

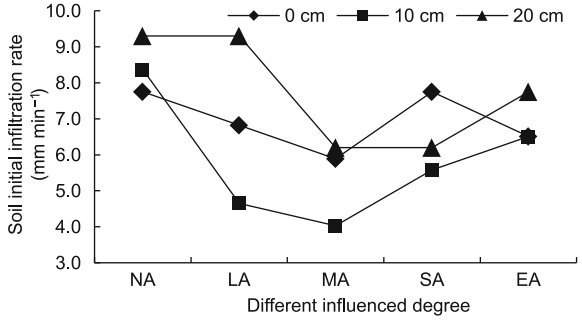

Figure 4 Variation of soil initial infiltration rates under different influenced degree.

2.2.2 *Variation of stable soil infiltration rates in different affected areas*

The vegetation readily developed a soil surface crust, reducing initial soil infiltration rates, and the variable distribution of soil organic matter was another factor which influenced changes in the initial soil infiltration rates. In conclusion, initial soil infiltration rates presented a similar changing trend in different soil layers and may be associated with the manner of cold alpine meadow degradation.

The formation of the thermokarst lake had a significant influence on stable soil infiltration rates, as shown in Figure 5. With the degree of impact intensifying, stable soil infiltration rates increased gradually in the topsoil, and their value at EA increased by 58.1% compared to NA. However, the changing trends in stable soil infiltration rates all declined at first and then increased at soil depths of 10–20 cm, reaching minimum values at MA. While the maximum value was 1.92 mm min^{-1} at NA, it was just 1.12 mm min^{-1} at MA at a depth of 10 cm. Meanwhile, there were no obvious changes in stable soil infiltration rates at a depth of 20 cm, its values ranging between 1.43 and 1.67 mm min^{-1}.

In general, the relation between stable soil infiltration rates and the degree of thermokarst lake influence is demonstrated as an exponential function of the topsoil. The regression equation can be expressed as

$$Y_1=1.101e^{0.006X}, \quad (1)$$

where Y_1 is the value of stable soil infiltration rate (mm min^{-1}), and X is the ecological variability index (%). In contrast, the relations were demonstrated as quadratic polynomial functions on the subsurface soil, the regression equations being expressed as

$$Y_2=0.0005X^2-0.0524X+2.4467, \quad R_2^2=0.97, \quad (2)$$

$$Y_3=0.0001X^2-0.0138X+1.7971, \quad R_3^2=0.94, \quad (3)$$

where Y_2, Y_3 are the values of stable soil infiltration rate at a depth of 10 and 20 cm, respectively. X is the ecological variability index (%)

The results show that the surface soil infiltration mechanism is different from that found in the subsurface. As shown in Tables 2 and 3, we found that stable soil infiltration had a higher correlation coefficient with soil bulk density, and the content of clay, silt, and sand (P<0.05). Although the soil bulk density gradually increased with the degree of the thermokarst lake impact intensifying, the soil hydraulic conductivity was enhanced, the main reason being that sandy soil has high permeability. However, roots of cold alpine meadow flora hindered the soil infiltration processes. Below a soil depth of 10 cm, roots were tiny, their function on soil hydraulic conductivities turned into promoting from inhibitory action of the topsoil, so the stable soil infiltration rates gradually declined from NA to MA. With the degree of impact intensifying, the influence of roots weakened soil hydraulic conductivity, the variation in stable soil infiltration rates being determined by the properties

Table 3 Correlation analysis of soil infiltration characteristics and soil physical properties[a)]

Correlation coefficient	Initial *f*	Stable *f*	Cumulative *f*	Soil moisture	Soil bulk density	Clay	Silt	Sand
Initial *f*	1							
Stable *f*	0.425	1						
Cumulative *f*	0.219	0.872**	1					
Soil moisture	0.415	−0.004	−0.04	1				
Soil bulk density	−0.135	0.473*	0.607*	−0.288	1			
Clay	0.160	−0.494*	−0.657**	0.229	0.754**	1		
Silt	0.099	−0.502*	−0.609**	0.195	−0.718**	0.899**	1	
Sand	−0.128	0.498*	0.696**	−0.177	0.754**	−0.947**	−0.900**	1

a) ** A statistical significance at $P \leqslant 0.01$; * a statistical significance at $P \leqslant 0.05$.

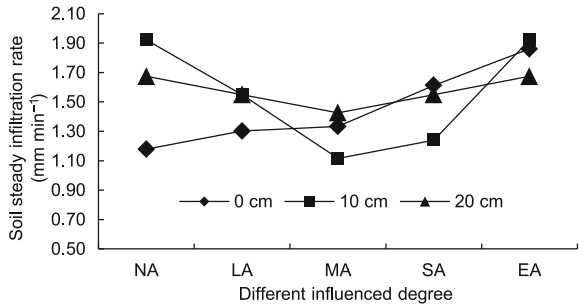

Figure 5 Variation of soil steady infiltration rates under different influenced degree.

of the soil types. At a soil depth of 20 cm, however, stable soil infiltration rates were controlled mainly by the structure of the soil pores, so variation in stable soil infiltration was weak.

2.2.3 The variation of cumulative soil infiltration in different affected areas

We analyzed the data of cumulative soil infiltration at the end of a period of 81 min. The results show large differences in all kinds of areas; the values were between 130.82 and 210.18 mm, as shown in Figure 6. With the degree of impact intensifying, soil cumulative infiltration underwent an increasing trend on the soil surface; the value of soil cumulative infiltration on EA increased by 59.1% compared with NA, whereas that of MA was slightly lower than LA. At a soil depth of 10 cm, the changing trends of soil cumulative infiltration decreased at first and then increased, the minimum value being 136.09 mm (SA) and the maximum 210.18 mm (EA), an increase of 19.8% compared to NA. At the 20 cm soil depth, the changing trend was similar to that at 10 cm, also reaching the minimum value at SA (130.82 mm); no differences in soil cumulative infiltration were found between NA and EA.

In conclusion, the formation of the thermokarst lake changed the rate of soil cumulative infiltration with time gradually increasing in the topsoil, but decreasing at first and then increasing in the subsurface, the changing trends being similar to stable soil infiltration rates. Combining this with Table 3, we found that the correlation coefficient between cumulative infiltration and stable soil infiltration

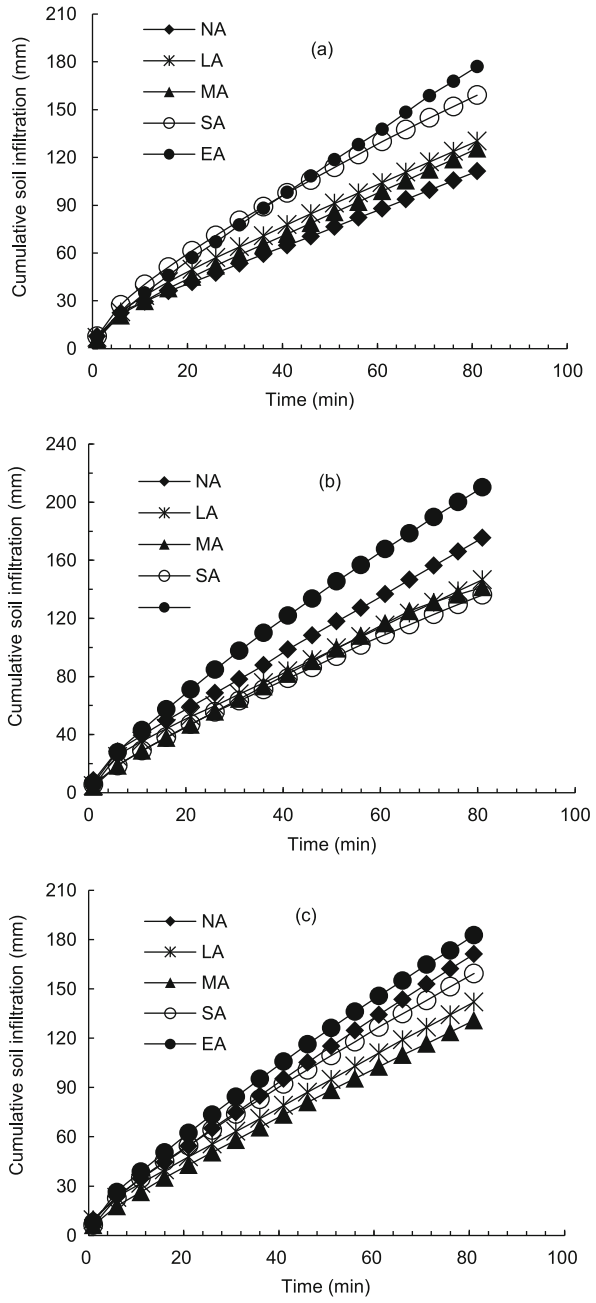

Figure 6 Variation of cumulative soil infiltration under different influenced degree.

rates reached 0.872 (P<0.01). Cumulative infiltration was also closely correlated with soil particle size distribution which characterizes soil texture. In brief, soil infiltration capacity was controlled mainly by soil texture in different affected areas of the thermokarst lake; soil texture affected the driving forces of soil water movement and hydraulic conductivity by acting on the surface energy of the soil particles, the size and the distribution of the soil pores and other factors (Xi et al. 2008). The formation of the thermokarst lake reduced soil water retention, with much water moving into the soil body, so reducing surface runoff in periods of plentiful rainfall. As the carrier of energy, the infiltration processes inserted much energy into the permafrost ecosystem and the weakened stability of the alpine meadow ecosystem.

2.3 Simulation of analyses of soil infiltration processes

In order to study the processes of soil infiltration and changes over time, researchers have established many infiltration models, including the Kostiakov model (Kostiakov, 1932), the General Empirical model (Jiang et al., 1986), the Horton model (Horton, 1940), and the Green-Ampt model (Green and Ampt, 1911), among others. This study used the above models to simulate soil infiltration processes under the impact of the thermokarst lake in order to test their applicability and accuracy.

(i) Kostiakov model. The general form of the infiltration equation given by Kostiakov is

$$f(t)=at^{-b}, \tag{4}$$

where $f(t)$ is the soil infiltration rate (mm min^{-1}), t is time (min), a and b are model parameters by test fitting.

(ii) General Empirical model. Jiang and Huang developed an empirical model expressed mathematically as

$$f(t)=a+bt^{-n}, \tag{5}$$

where $f(t)$ is the soil infiltration rate (mm min^{-1}), t is time (min), a and b are model parameters by test fitting.

(iii) Horton model. Horton developed an infiltration equation:

$$f(t)=f_c+(f_0-f_c)e^{-k}, \tag{6}$$

where $f(t)$ is the soil infiltration rate (mm min^{-1}), t is time (min), f_c is the stable state value of f, f_0 is the initial state value of f, and k is the infiltration decay factor.

(iv) Green-Ampt model. Green and Ampt presented a model based on the assumption that soil may be regarded as a bubble of tiny capillary tubes irregular in area, direction, and shape, with their infiltration equation taking the following form:

$$f(t)=at^{-1/2}+f_c, \tag{7}$$

where $f(t)$ is the soil infiltration rate (mm min^{-1}), t is time (min), f_c is the stable state value of f, and a is the model parameter of test fitting.

In the Kostiakov model, a is the value of initial infiltration rate and b is the degree of infiltration rate decreasing with time. The results of fitting showed that parameter a was between 4.151 and 8.841, but larger values at NA and EA were achieved at different soil depths, which were similar to the observed results. Parameter b was between 0.263 and 0.517, but larger values at NA and LA were achieved, all showing that a higher vegetation cover in cold alpine meadow could block soil infiltration effectively. a was the value of the stable infiltration rate. Parameter b also influenced the initial soil infiltration rate and attained a positive relation with it. Parameter n was a reduced gradient from initial infiltration to stable infiltration. The simulated results show that parameter a was between 0.592 and 1.773, b was between 3.023 and 7.845, and n was between 0.363 and 1.151. Stable soil infiltration rates simulated by the General Empirical model revealed considerable differences when compared with the observed values. The Horton model can be used to simulate initial soil infiltration rate and stable infiltration rate. Our results showed that f_0 was between 1.286 and 4.162, and f_c was between 1.286 and 4.162. However, simulated results of the initial soil infiltration rates were higher than observed but they indicated a similar changing trend. Finally, the Horton model was found to have certain accuracy for the simulated result of stable soil infiltration. In the Green-Ampt model parameter a was between 3.357 and 7.815, and f_c was between 0.040 and 1.1556, but all of the simulated results of parameters a and f_c were less than the observed values.

In order to evaluate the imitative effect of different models of soil infiltration processes on cold alpine meadow, we undertook a statistical analysis of the determination coefficient (R^2) of regression equations, as shown in Figure 7. It turned out that the values of R^2 were all higher in the study area, and the imitative effect had similar trends at different soil depths. On the soil surface, the Horton model results were better than when the influence of impact degree of the thermokarst lake was light; the values of R^2 reached more than 0.997. With the degree of impact intensifying, the imitative effect of the Horton model was gradually reduced, but the results of the General Empirical model were different, the multiple correlation coefficient reaching more than 0.992. In addition, the Kostiakov and Green-Ampt models were unable to generate better results. At the 10 cm soil depth, all models failed to produce a desirable outcome for LA and MA, but they simulated better the soil infiltration processes at SA and EA. Two main reasons explain these results. First, the roots of the higher vegetation coverage were denser and showed a slight disturbance of the soil structure when the topsoil was removed. Second, the distribution of the soil edaphon and insect nests also added a negative impact. At a soil depth of 20 cm, the simulated results of the Horton and General Empirical models were more acceptable than the others listed above.

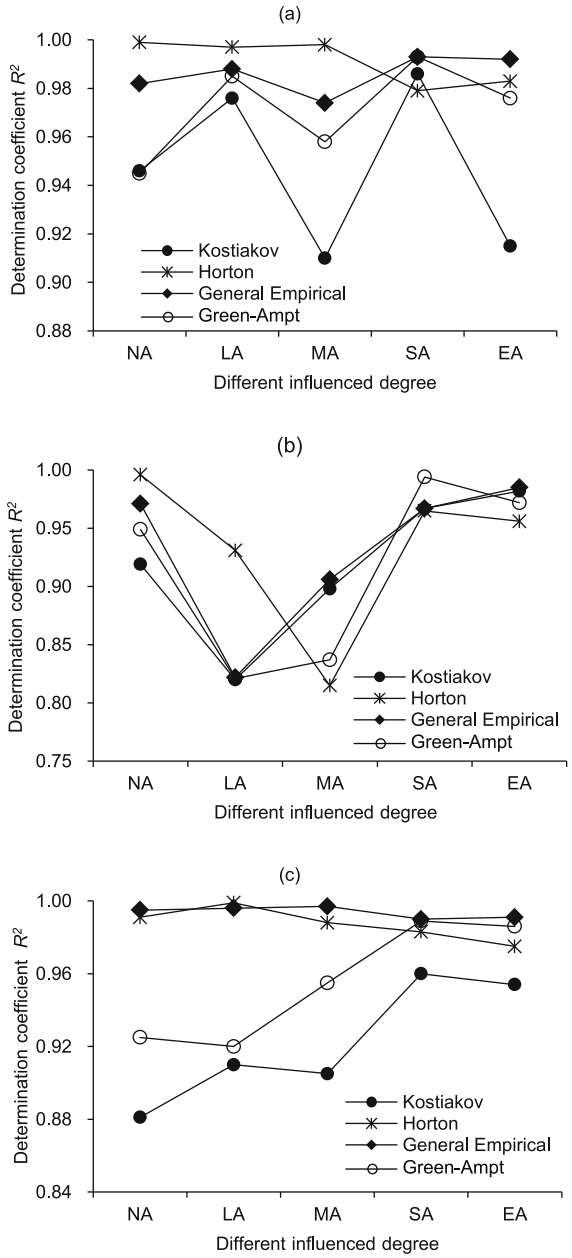

Figure 7 Comparison of the determination coefficient of different soil infiltration models. (a) 0 cm; (b) 10 cm; (c) 20 cm.

Based on the simulated results, the observed results and the multiple correlation coefficients mentioned above, it is shown that the Horton model was able to generate more successfully the effect on soil infiltration processes in cold alpine meadow. With the degree of impact intensifying, the changing trends of parameters f_0, f_c, k display an initial increase and then a decrease, a trend similar to the observed results.

The soil infiltration processes in the cold alpine meadow biome are influenced by precipitation elements, different cover conditions, soil properties, permafrost characteristics, and other factors. They are complicated by hydrological processes coupled with a multi-factor effect. Water infiltration capacity determines the amount of soil surface runoff during torrential rain and the extent of the risk of soil erosion. In addition, it influences variations in soil moisture and groundwater, the transformation of interflow and underground runoff. The formation of the thermokarst lake studied here caused degradation of the alpine soil, a decline in the coverage of cold alpine meadow, replacement of the original vegetation of *kobresia* and *wild grass* by ruderal species, decline in the soil water-holding capacity and an enhanced hydraulic conductivity ability. So, soil dried more quickly and, at the same time, altered the soil infiltration properties. With the degree of impact intensifying, initial soil infiltration rates decreased, but stable infiltration rates and cumulative infiltration all increased in the natural state, the values of soil infiltration characteristics undergoing a changing trend of parabolic style on the subsurface. It has been reported that, when air temperature rises by 2°C, the cold alpine meadow system distributed in the lower mountains and planar terrains from the Kunlun Mountains to Anduo will suffer a moderate to light degradation in most areas, but local areas are likely to suffer serious degradation in the next 50 a (Wang et al., 2006). Clearly, thermokarst lakes are an important factor in alpine soil degradation, changes in soil infiltration processes in its vulnerable areas and a decline in the generation of runoff. When soil loses the protection of a vegetation cover, the intensity of erosion by water, freeze-thaw stress, and wind increases, thus undermining the stability of the cold alpine meadow system.

3 Conclusions

The therrmokarst lake caused changes in the cold alpine meadow system; this involved variation in soil physical properties, together with a decrease in the distribution of soil porosity, increasingly coarse particle sizes on sites disrupted to varying degrees, and thus facilitating the loss of soil moisture.

With the degree of impact intensifying, initial soil infiltration rates declined, the greatest decrease being in moderately affected areas; the values showed a close correlation with initial soil moisture content. Moreover, a stable soil infiltration rate was controlled mainly by soil texture and the relation between the stable soil infiltration rates and the impact degree of thermokarst lake was clearly demonstrated as an exponential function on the topsoil, but that was demonstrated as a quadratic polynomial on the subsurface.

With the degree of impact intensifying, soil cumulative infiltration increased gradually on the soil surface in the study area, but decreased initially and then increased on the subsurface, mainly controlled by the stable soil infiltration rates together with a negative correlation with the clay content and a positive correlation with the silt and sand content.

The Horton model was able to generate better results on

soil infiltration processes of the cold alpine meadow when influenced by the thermokarst lake. With the degree of impact intensifying, the changing trends of the three parameters f_0, f_c, k initially increased and then decreased, which is similar to the observed results. Finally, it was readily ascertained that the stable infiltration stage occurred in moderately affected terrain.

We thank the anonymous reviewers for their comments. This work was supported by the National Natural Science Foundation of China (Grant No. 41271092), the National Basic Research Program of China (Grant Nos. 2010CB951402, 2012CB026101), and the Key Project of the National Natural Science Foundation of China (Grant No. D010102-91125010).

Green W H, Ampt G A. 1911. Studies on soil physics, flow of air and water through soil. J Agr Sci, 76: 1–24

Grosse G, Romanovsky V, Walter A K, et al. 2006. Distribution of thermokarst lakes and ponds at three Yedoma sites in Siberia. 9th International Conference on Permofrost. 551–556

Guo D L, Wang H J. 2012. A projection of permafrost degradation on the Tibetan Plateau during 21st century. J Geophys Res, 117: D05106

He Y, Wu Y F, Liu Q F. 2012. Vulnerability assessment of areas affected by Chinese cryospheric changes in future climate change scenarios. Chin Sci Bull, 57: 4784–4790

Hinzman L D, Goering D J, Li S, et al. 1997. Numeric simulation of thermokarst formation during disturbance. Disturbance and Recovery in Arctic Lands: An Ecological Perspective. Dordrecht: Kluwer Academic Publishers. 191–211

Horton R E. 1940. An approach toward a physical interpretation of infiltration-capacity. Soil Sci Am Proc, 5: 399–417

Jiang D S, Huang G J. 1986. Study on the filtration rate on soils on the Loess Plateau of China (in Chinese). Acta Pedol Sin, 23: 299–305

Johanna M K, Steve W L, Georgia D. 2012. Thermokarst lake, hydrological flow and water balance indicators of permafrost change in Western Siberia. J Hydrol, 464-465: 459–466

Jones B M, Grosse G, Arp C D, et al. 2011. Modern thermokarst lake dynamics in the continuous permafrost zone, northern Seward Peninsula, Alaska. J Geophys Res, 116: G00M03

Kokelj S V, Jorgenson M T. 2013. Advance in thermokarst research. Permafrost Periglac Proc, 24: 108–119

Kostiakov A N. 1932. On the dynamics of the coeffient of water percolation in soil and on the necessity of studing it froma dynamic point of view for purposes of amelioration. Moscow: Translation of the 6th Conference of the International Society for Soil Sciences, Part A. 17–21

Li Z, Liu Y H, Yang Q. 2011. Review on effects mechanism of soil water infiltration (in Chinese). J Irrig Drain, 30: 124–130

Lin Z J, Niu F J, Xu J, et al. 2009. The effect of embankment construction on permafrost in the Tibetan Plateau (in Chinese). J Glaciol Geocryol, 31: 1127–1136

Lin Z, Niu F, Xu Z, et al. 2010. Thermal regime of a thermokarst lake and its influence on permafrost, Beiluhe Basin, Qinghai-Tibet Plateau. Permafrost Perigl Proc, 21: 315–324

Ma W, Mu Y H, Li G Y, et al. 2013. Responses of embankment thermal regime to engineering activities and climate change along the Qinghai-Tibet Railway (in Chinese). Sci Sin Terrae, 43: 478–489

Nan Z T, Li S X, Cheng G D. 2005. Prediction of scenario of permafrost distribution on the Qinghai-Tibet Plateau in the next 50 and 100 years. Sci China Ser D-Earth Sci, 48: 797–804

Niu F, Lin Z, Liu H, et al. 2011. Characteristics of thermokarst lakes and their influence on permafrost in Qinghai-Tibet Plateau. Geomorphology, 132: 222–233

Pan B T, Li J J. 1996. Qinghai-Tibetan Plateau: A driver and amplifier of the global climate change III. The effects of the uplift of Qinghai-Tibetan Plateau on climate changes (in Chinese). J Lanzhou Univ (Nat Sci), 32: 108–115

Ren J W. 2013. Updating assessment results of global cryospheric change from SPM of IPCC WGI fifth assessment report (in Chinese). J Glaciol Geocryol, 35: 1065–1067

Sergey A, Zimov, Edward A G, et al. 2006. Permafrost and the global carbon budget. Science, 312: 1612–1613

Shen B, Huang H H. 2008. The Principle of Hydrology (in Chinese). Beijing: China Waterpower Press

Walter K M, Edwards M E, Grosse G, et al. 2007. Thermokarst lakes as a source of atmospheric CH_4 during the Last Deglaciation. Science, 318: 633–636

Walter K M, Zimov S A, Chanton J P, et al. 2006. Methane bubbling from Siberian thaw lakes as a positive feedback to climate warming. Nature, 443: 71–75

Wang G X, Li Y S, Wu Q B, et al. 2006. Impacts of permafrost changes on alpine ecosystem in Qinghai-Tibet Plateau. Sci China Ser D-Earth Sci, 49: 1156–1169

Wang G X, Wang Y B, Li Y S, et al. 2007. Influences of alpine ecosystem responses to climate change on soil properties on Qinghai-Tibet Plateau, China. Catena, 70: 506–514

Wang Y B, Wu Q B, Niu F J. 2011. The impact of Thermokarst lake formation on soil environment of alpine meadow in permafrost regions in the Beiluhe basin of the Tibetan Plateau (in Chinese). J Glaciol Geocryol, 33: 659–667

Wu Q B, Niu F J. 2013. Permafrost changes and engineering stability in Qinghai-Xizang Plateau. Chin Sci Bull, 58: 1079–1094

Xi H Y, Feng Q, Cheng Y F, et al. 2008. Permeability characteristics of soils and their dependence on soil condition in Ejina Oasis (in Chinese). J Glaciol Geocryol, 30: 976–982